

# Nanobody Targeting of Epidermal Growth Factor Receptor (EGFR) Ectodomain Variants Overcomes Resistance to Therapeutic EGFR Antibodies



Joseph Tintelnot<sup>1</sup>, Natalie Baum<sup>1</sup>, Christoph Schultheiß<sup>1</sup>, Friederike Braig<sup>1</sup>, Marie Trentmann<sup>1</sup>, Johannes Finter<sup>2</sup>, William Fumey<sup>3,4</sup>, Peter Bannas<sup>4</sup>, Boris Fehse<sup>5</sup>, Kristoffer Riecken<sup>5</sup>, Kerstin Schuetze<sup>3,4</sup>, Carsten Bokemeyer<sup>1</sup>, Thies Rösner<sup>6</sup>, Thomas Valerius<sup>6</sup>, Matthias Peipp<sup>6</sup>, Friedrich Koch-Nolte<sup>3</sup>, and Mascha Binder<sup>1</sup>

## Abstract

Epidermal growth factor receptor (EGFR) ectodomain variants mediating primary resistance or secondary treatment failure in cancer patients treated with cetuximab or panitumumab support the need for more resistance-preventive or personalized ways of targeting this essential pathway. Here, we tested the hypothesis that the EGFR nanobody 7D12 fused to an IgG1 Fc portion (7D12-hcAb) would overcome EGFR ectodomain-mediated resistance because it targets a very small binding epitope within domain III of EGFR. Indeed, we found that 7D12-hcAb bound and inhibited all tested cell lines expressing common resistance-mediating EGFR ectodomain variants. Moreover, we assessed receptor functionality and binding properties in synthetic mutants of the 7D12-hcAb epitope to model resistance to 7D12-hcAb. Because the 7D12-hcAb epitope almost completely overlaps with the EGF-binding site, only position R377 could be mutated without

simultaneous loss of receptor functionality, suggesting a low risk of developing secondary resistance toward 7D12-hcAb. Our binding data indicated that if 7D12-hcAb resistance mutations occurred in position R377, which is located within the cetuximab and panitumumab epitope, cells expressing these receptor variants would retain sensitivity to these antibodies. However, 7D12-hcAb was equally ineffective as cetuximab in killing cells expressing the cetuximab/panitumumab-resistant aberrantly N-glycosylated EGFR R521K variant. Yet, this resistance could be overcome by introducing mutations into the Fc portion of 7D12-hcAb, which enhanced immune effector functions and thereby allowed killing of cells expressing this variant. Taken together, our data demonstrate a broad range of activity of 7D12-hcAb across cells expressing different EGFR variants involved in primary and secondary EGFR antibody resistance.

## Introduction

Monoclonal antibodies (mAb) directed against the epidermal growth factor receptor (EGFR) have become one of the mainstays of targeted therapy in metastatic colorectal cancer

(mCRC) and head and neck squamous cell carcinoma (HNSCC; refs. 1, 2). Two EGFR-directed antibodies are currently in routine clinical application (1, 3–5). Both the IgG1 antibody cetuximab and the IgG2 antibody panitumumab target large epitopes that partially overlap with each other as well as with the EGF-binding site in domain III of the receptor. These antibodies inhibit ligand binding and receptor dimerization resulting in the inhibition of downstream signaling, cell-cycle arrest, and induction of apoptosis (6). In addition to interference with downstream signaling, cetuximab induces immune responses via antibody-dependent cellular cytotoxicity (ADCC) by natural killer (NK) cells (7), whereas panitumumab's IgG2 isotype mainly engages myeloid cells such as neutrophils and monocytes through FcγRIIa (8). The second mechanism of immune effector functions is complement-dependent cytotoxicity (CDC), which apparently cannot be induced by cetuximab or panitumumab alone, but by combinations of EGFR antibodies with different epitope fine specificities *in vitro* (9).

All of these mechanisms critically rely on intact binding sites on EGFR that allow the therapeutic antibody to recognize its target. Because cancer generally evolves by an iterative process of genetic diversification and clonal evolution under the selective pressure of therapeutic challenge (10, 11), EGFR epitope

<sup>1</sup>Department of Oncology and Hematology, BMT with section Pneumology, University Medical Center Hamburg-Eppendorf, Hamburg, Germany. <sup>2</sup>Department of Pediatrics, Center for Obstetrics and Pediatrics, University Medical Center Hamburg-Eppendorf, Hamburg, Germany. <sup>3</sup>Institute of Immunology, University Medical Center Hamburg-Eppendorf, Hamburg, Germany. <sup>4</sup>Department of Diagnostic and Interventional Radiology and Nuclear Medicine, University Medical Center Hamburg-Eppendorf, Hamburg, Germany. <sup>5</sup>Research Department Cell and Gene Therapy, Department of Stem Cell Transplantation, University Medical Center Hamburg-Eppendorf, Hamburg, Germany. <sup>6</sup>Division of Stem Cell Transplantation and Immunotherapy, Department of Internal Medicine II, Christian-Albrechts-University Kiel, Kiel, Germany.

**Note:** Supplementary data for this article are available at Molecular Cancer Therapeutics Online (<http://mct.aacrjournals.org/>).

**Corresponding Author:** Mascha Binder, University Medical Center Halle, Department of Internal Medicine IV, Ernst-Grube-Str. 40, 06120 Halle (Saale), Germany. Phone: (0345) 557 2924; Fax: (0345) 557 2950; E-mail: Mascha.Binder@uk-halle.de

**doi:** 10.1158/1535-7163.MCT-18-0849

©2019 American Association for Cancer Research.

escape variants that preserve receptor functionality are to be expected during EGFR-targeted treatment. Indeed, a growing body of evidence demonstrates that despite the large binding sites of the two licensed EGFR antibodies, single replacement mutations may compromise antibody binding. Such mutant receptors are functionally intact and can be found in tumor material or circulating tumor DNA from patients resistant to EGFR antibodies, thus representing an evasive mechanism to targeted therapy. In recent clinical studies, EGFR ectodomain mutations at position V441, S442, R451, I462, S464, G465, K467, K489, I491, and S492 were reported. Mutations at indicated positions—with the exception of R451—led to decreased antibody binding, thus resulting in clinical resistance (12–15). As expected, it depends on the precise position of the missense mutation in relation to the respective antibody epitope, whether binding of cetuximab, panitumumab, or both antibodies is lost (16). In colorectal cancer, acquired resistance due to such epitope escape variants appears to be a rather common phenomenon in selected cohorts with resistant tumors (13, 15, 17). In fact, the frequencies reported in the literature are somewhat biased due to different detection technologies and inhomogeneous patient cohorts. Some of the mutations seem, however, to be more frequent than others. Whereas EGFR S492R or G465R each are detected in approximately 20% of patients with clinical resistance, none of the other known mutations accounts for more than 10% of cases in resistant cohorts (12, 13, 15, 17).

In addition, our group recently described an *EGFR* single-nucleotide polymorphism (SNP) at position 521 (R521K) that is present in approximately one third of HNSCC patients and that confers cetuximab resistance in this setting (18–21). Interestingly, this SNP is not located within the cetuximab-binding site, but on the opposite face of EGFR domain III. Therefore, a direct epitope escape effect of this variant appeared unlikely, and we found differential EGFR glycosylation patterns to be responsible for impaired cetuximab affinity and reduced effectivity in tumors expressing this receptor variant (18). Of note, due to impaired antibody affinity, cetuximab did not inhibit the EGFR pathway in cells expressing the EGFR R521K variant, but its binding affinity was sufficient to mediate ADCC, at least when its Fc part was optimized for ADCC induction.

Taken together, EGFR ectodomain variants limit the benefit of EGFR-targeting antibodies in a substantial proportion of patients both as primary and acquired mechanisms of resistance. We and others have therefore sought strategies to prevent or overcome resistance, e.g., by use of EGFR antibody mixtures targeting different epitopes (MM-151 and Sym004; refs. 22, 23), rational antibody switching upon resistance (14), or use of antibodies with improved immunologic effector functions to retain efficacy in "low-affinity" EGFR variants (18).

Another potential resistance-preventive strategy would be the development of moieties targeting very small binding interfaces on the EGFR that completely overlap with the EGF-binding site. *In vivo* selection of resistance-mediating mutations against these moieties would clearly be discouraged due to loss of EGF-binding and thereby disrupted receptor functionality. Here, we provide evidence that the antigen-binding domain of heavy-chain-only antibodies from camelids (24), so-called nanobodies, may provide such desirable characteristics (25, 26). The nanobody 7D12, which was previously reported to sterically inhibit EGF binding,

binds to a very small epitope that almost exclusively consists of amino acids functionally relevant for EGF binding (27, 28). We show that 7D12, fused to a human Fc portion (ref. 29; 7D12-hcAb), is able to bind and block EGFR with all tested acquired resistance mutations and—if Fc-engineered—may boost ADCC/Fc-mediated effector functions also in EGFR variants with low affinity to conventional EGFR antibodies or downstream on *ras* sarcoma gene (*RAS*) mutated clones, rendering it an attractive candidate for future clinical development.

## Materials and Methods

### EGF and antibody binding

Essential amino acid positions that lead to loss of EGF, cetuximab, panitumumab, or nanobody 7D12 binding to the EGFR were taken from the literature or from our own previously published data (Table 1). The 3D structure of domain III of the EGFR (Fig. 1) was extracted from Protein Data Bank (1IVO). Binding of EGF, antibodies, and nanobody was visualized using the PyMol Molecular Graphics System, Version 1.7.4.5 Schrödinger, LLC.

### Cell lines

The human cell line SAT was kindly provided by M. Baumann in 2006 (University of Dresden, Germany), and the cell line UTSCC-14 was kindly provided by R. Grenman in 2011 (University of Turku, Finland). Both lines were cultivated in DMEM (Life Technologies) supplemented with 10% (v/v) FBS (Merck Millipore) and 1% (v/v) penicillin/streptomycin (Gibco/Life Technologies) at 37°C in a humidified atmosphere including 5% CO<sub>2</sub>. Ba/F3 cells (CSC-C2045, Creative Bioarray) were kindly provided by Stefan Horn (UKE) in 2014 and were maintained in RPMI medium containing 10% (v/v) FBS, 1% (v/v) penicillin/streptomycin, and 10 ng/mL recombinant murine IL3 purchased from PeproTech. *Mycoplasma* testing was done in June 2016 (Venor-GeM kit, Merck). For experiments, cells were used at passages 3–15 after thawing.

### Cloning of EGFR expression constructs

For ectopic expression of the complete human wild-type (WT) EGFR, the respective full-length cDNA was inserted into a third-generation, self-inactivating (SIN) lentiviral gene ontology vector LeGO-iG3-Puro+/eGFP as well as LeGO-iG3-Puro+/mCherry, as described previously (12, 30). The EGFR mutants S492R, I491K, K489E, K467T, G465R, S464L, I462A, R451C, V441F, D379A, and R377A were generated from the WT construct in the pcDNA3.1(+) vector with the QuikChange XL Site-Directed Mutagenesis Kit (Agilent Technologies) as described in ref. 12. The respective EGFR mutant was amplified using individually designed oligonucleotides (Supplementary Table S1) and cloned into the LeGO-iG3-Puro+/eGFP vector by In-Fusion HD Cloning Plus (Takara Bio). The gene encoding *hKRAS* bearing an oncogenic mutation GGT>GTT that leads to the amino acid substitution G12V was amplified from human SW480 colorectal cancer cells and cloned into LeGO-iC2-Zeo+/mCherry. Vector maps and sequence data for all parental vectors are available at <http://www.LentiGO-Vectors.de>.

### Cell transduction with EGFR expression constructs

Ba/F3 cells were lentivirally transduced with WT or mutant *EGFR* encoding vector. For some experiments, *EGFR* WT-transduced

**Table 1.** Overview of EGFR ectodomain III variants and their impact on EGF and anti-/nanobody binding<sup>a</sup>

Position	EGF	7D12-hcAb	Cetuximab	Panitumumab
P373 (16)	N.e.	N.e.	↓	↓
V374 (47)	↓	N.e.	N.e.	↓
F376 (16)	N.e.	N.e.	↓	N.e.
R377 (16, 28) and this study	-	↓	-	-
D379 (16, 28, 47) and this study	↓	↓	↓	↓
F381 (16, 28)	↓	↓	-	-
P386 (16)	N.e.	N.e.	↓	↓
L406 (47)	↓	N.e.	N.e.	N.e.
Q408 (28, 48, 38)	↓	↓	↓	↓
W410 (16)	N.e.	N.e.	-	↓
P411 (16)	N.e.	N.e.	↓	↓
E412 (16)	N.e.	N.e.	↓	↓
R414 (16)	N.e.	N.e.	-	↓
T415 (16)	N.e.	N.e.	-	↓
Q432 (16, 48, 38)	↓	N.e.	↓	↓
H433 (16, 28, 48, 38)	↓	↓	↓	↓
F436 (47, 16)	N.e.	N.e.	↓	↓
V441 (15) and this study	-	-	↓	↓/-
S442 (15, 16)	N.e.	N.e.	-	-
R451 (13) and this study	N.e.	-	↓/-	↓/-
I462 (16, 47) and this study	-	-	↓	↓/-
S464 (13) and this study	-	-	↓	↓
G465 (13, 12) and this study	-	-	↓	↓
K467 (13, 16, 38) and this study	↓/-	-	↓/-	↓/-
K489 (16, 49, 50) and this study	↓/-	-	↓	↓
I491 (13, 49) and this study	-	-	↓	↓/-
S492 (13, 16, 38) and this study	-	-	↓	-
N497 (38)	↓	N.e.	-	-
R521 (18)	N.e.	N.e.	↓	↓

<sup>a</sup>Different amino acid positions of EGFR ectodomain D III and their influence on EGF-stimulated growth or EGF-binding and 7D12-hcAb, cetuximab, or panitumumab binding were extracted from the literature or from data derived in this study. Affinity loss was indicated with (↓) using a cutoff of about 30% binding reduction and noninfluencing was indicated with (-). N.e., not evaluated. Mutations acquired in patients during anti-EGFR therapy (gray) are marked.

Ba/F3 cells were further transduced with *hKRAS* (G12V). Virus production was described earlier (30). Effectively transduced cells were sorted based on their selectable fluorescent marker by fluorescence-activated cell sorting (FACS) on a FACSAria Illu (Becton Dickinson), and transduction efficiency was determined. Ba/F3 cell lines stably expressing EGFR WT or EGFR S492R, I491K, K489E, K467T, G465R, S464L, I462A, R451C, V441F, D379A, or R377A mutants were established by puromycin (1 µg/mL; InvivoGen) and Ba/F3 *hKRAS*/EGFR WT cells by puromycin and zeocin (100 µg/mL; InvivoGen) selection.

#### Nanobody generation

The coding sequence of nanobody 7D12 (27) was cloned into the pCSE2.5\_IgG1 expression vector upstream of the hinge, CH2 and CH3 domains of human IgG1 (kindly provided by Thomas Schirrmann, Yumab, Braunschweig, Germany; ref. 31). Coding sequence of E345R (32) 7D12-E-hcAb, and G236A-S239D-I332E (33) 7D12-T-hcAb mutated nanobody 7D12 was generated by Integrated DNA Technologies (IDT) and cloned according to 7D12. Recombinant nanobody-human IgG1 heavy-chain antibodies were expressed in HEK-6E cells and purified by affinity chromatography on protein A (34).

#### Antibody/nanobody binding

EGFR WT or EGFR S492R, I491K, K489E, K467T, G465R, S464L, I462A, R451C, V441F, D379A, and R377A mutated Ba/F3 cells were stained with polyclonal EGFR antibody (R&D Systems), therapeutic antibody, or nanobody-based heavy-chain antibodies, followed by appropriate fluorescently labeled secondary antibodies (R&D Systems) before flow cytometry on a FACSCanto

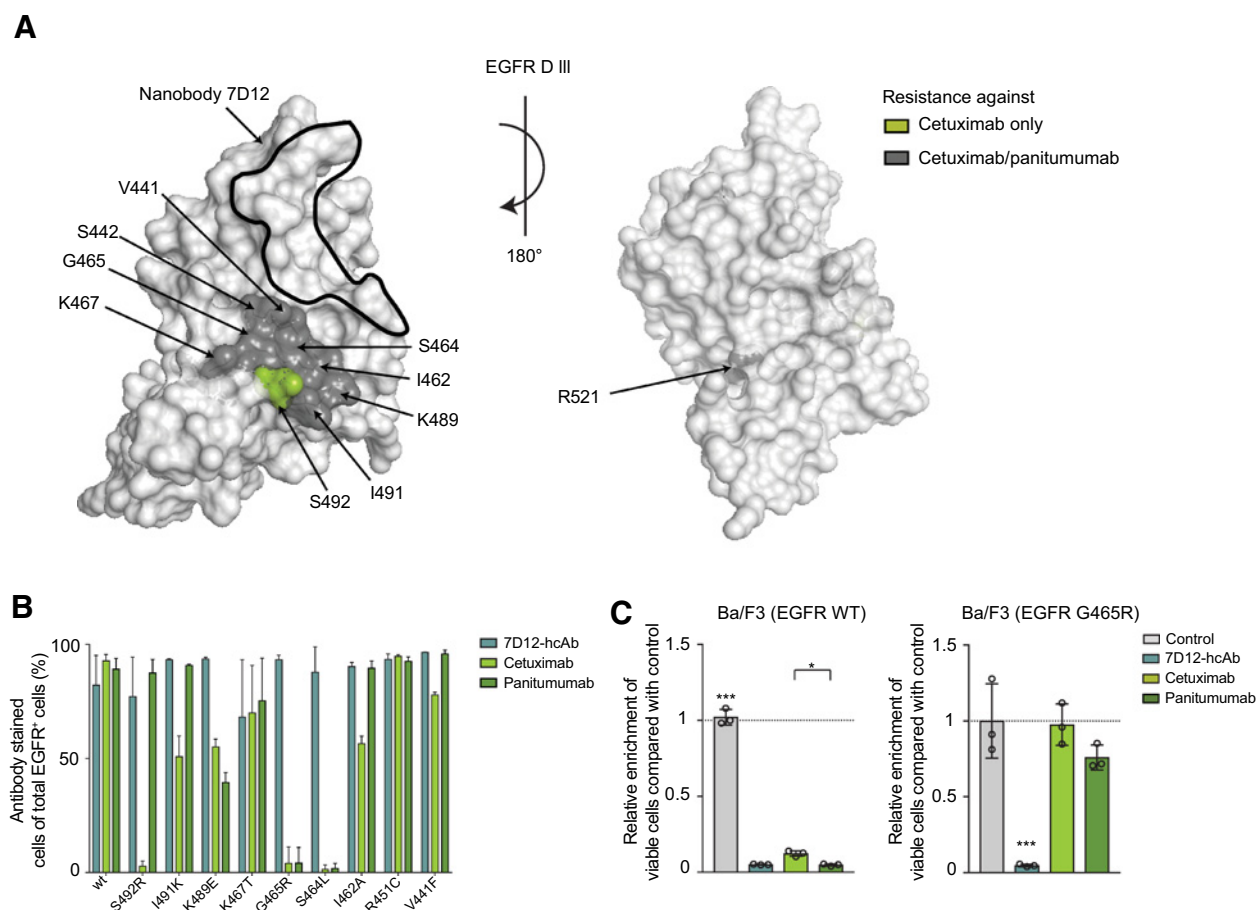
(Becton Dickinson). Percentages of monoclonal antibody/nanobody stained cells of total EGFR-positive cells were determined with FlowJo v.10.4 (Tree Star).

#### Cellular proliferation assays

Cetuximab (Merck) and panitumumab (Amgen) were obtained from the Hospital Pharmacy of the UKE and 7D12-hcAb was generated as described above. Ba/F3 cells transduced with EGFR WT or EGFR G465R were seeded in triplicate at equal densities of  $1.0 \times 10^6$  cell/mL and cultured in the absence or presence of EGF in combination with 5 µg/mL (32.8 µmol/L) cetuximab, 2.5 µg/mL (17 µmol/L) panitumumab, and 2.5 µg/mL (60 µmol/L) 7D12-hcAb or without as control. The average number of viable cells was measured after trypan blue staining using Vi-CELL Cell Viability Analyzer (Beckman Coulter) every 24 hours for 7 days. Ligand and therapeutics were added freshly every 24 hours.

#### EGFR-ligand-stimulated proliferation

Ba/F3 cells transduced for EGFR WT or EGFR S492R, I491K, K489E, K467T, G465R, S464L, I462A, R451C, V441F, D379A, or R377A-mutant expression were transformed to IL3 independence by subsequent culturing in the absence of IL3 and in the presence of 5 ng/mL EGF, or without growth factor (control). In some experiments, other EGFR ligands such as amphiregulin, betacellulin, epigen, or epiregulin at concentrations of 10 ng/mL were used. Over a time period of 4 days, EGF-dependent stimulation was determined daily by comparing increase in living cells using Vi-CELL Cell Viability Analyzer (Beckman Coulter) relative to unstimulated cells.

**Figure 1.**

Antibody and nanobody targeting of EGFR ectodomain III variants involved in resistance to cetuximab and panitumumab. **A**, Visualization of EGFR ectodomain mutations and nanobody 7D12 epitope. Domain III (D III) of the EGFR was extracted under accession code 1IVO from Protein Data Bank. Single amino acid mutations that lead either to abrogation of both panitumumab or cetuximab binding (dark gray) or cetuximab binding only (green) were marked and the nanobody epitope was circled (black). **B**, Nanobody 7D12-hcAb binds to EGFR-mutant Ba/F3 cells. Cells of EGFR WT and EGFR-mutant transduced Ba/F3 cells were fluorescently labeled with either EGFR and/or nanobody 7D12-hcAb (blue) therapeutic antibody cetuximab (light green) or panitumumab (dark green) and specific secondary antibody. Relative amount of EGFR<sup>+</sup> cells was determined by gating on EGFR-positive cells followed by gating on antibody/nanobody-labeled cells. Experiments were performed at least two times as triplicates. Results are presented as mean  $\pm$  SD. **C**, Nanobody 7D12-hcAb blocks proliferation of EGFR-mutant Ba/F3 cells. Proliferation after 4 days of EGF stimulation was determined for EGFR WT (left) and EGFR G465R (right)-transduced Ba/F3 cells by comparing increase of viable cells after antibody or nanobody treatment to EGF treatment alone (control). Results are shown for treatment with nanobody 7D12-hcAb 60  $\mu$ mol/L (blue), antibody cetuximab 32.8  $\mu$ mol/L (light green), or panitumumab 17  $\mu$ mol/L (dark green) as mean  $\pm$  SD. Experiments were performed two to three times in triplicates. Statistical significance was calculated using one-way ANOVA followed by a Tukey *post hoc* test for multiple comparisons (**C**). \*,  $P < 0.05$ ; \*\*\*,  $P < 0.001$ .

### Random peptide phage display library screening on nanobody 7D12-hcAb

The linear 12-mer and the cyclic 7mer random peptide library were purchased from New England Biolabs. Screenings were performed after 2-fold negative selection on polyclonal immunoglobulin G (IgG; Octapharma) on 7D12-hcAb and rituximab as control antibody, phage enrichment was monitored over the selection rounds as suggested by the supplier, and phage insert deep sequencing was performed using amplification primers ACACCTCTTTCCCTACACGACGCTCTTCCGATCTTATTCGCAATTCCTTTAGTG and TGACTGGAGTTCAGACGTGTGCTCTTCCGATCTGCCCTCATAGTTAGCGTAACG followed by barcoding primers AATGATACGGCGACCACCGAGATCTACACTCTTTCCCTACACGACGCTC and CAAGCAGAAGACGGCATACGAGAT(N<sub>6-7</sub>)

GTGACTGGAGTTCAGACGTGTG on an Illumina MiSeq (Illumina) essentially as described earlier (12, 18). Enriched amino acid sequences were aligned to specific protein sequences and sequences that were already enriched (>1) in baseline library were excluded using RStudio v.1.0.143 (RStudio Inc.) and R programming language (R Development Core Team). Nanobody or antibody motifs were analyzed using Gapped Local Alignment of Motifs 2 (GLAM2) with default settings according to (35).

### Spheroid assay

UTSCC-14 or SAT cells were washed and suspended in DMEM containing 10% FBS, 1% penicillin/streptomycin, 5 ng/mL EGF, and 2% Matrigel Growth Factor Reduced (GFR) Basement Membrane Matrix or without GFR as control. Cell suspension was

seeded in 96-well plate and centrifuged at  $1,000 \times g$  for 10 minutes at  $4^{\circ}\text{C}$ . Pictures were taken every other day with  $10\times$  magnification using Axiovert 25 microscope and AxioCamMRC (Carl Zeiss). Cell size was calculated using AxioVision v4.9. (Carl Zeiss). After 7 days of culture  $100\ \mu\text{L}$  medium containing  $5\ \mu\text{g}/\text{mL}$  ( $32.8\ \mu\text{mol}/\text{L}$ ) cetuximab,  $2.5\ \mu\text{g}/\text{mL}$  ( $17\ \mu\text{mol}/\text{L}$ ) panitumumab,  $2.5\ \mu\text{g}/\text{mL}$  ( $60\ \mu\text{mol}/\text{L}$ ) 7D12-hcAb or medium alone as control were added. The medium was changed every other day, and spheroid size was calculated until day 13 was reached.

#### CDC assay

Human UTSCC-14, SAT, Ba/F3 EGFR WT, Ba/F3 EGFR R521K, or Ba/F3 EGFR WT/KRAS (G12V) cells were washed and resuspended in PBS containing 0.2% BSA. Cells (50,000) were seeded in a total volume of  $200\ \mu\text{L}$  in 96-well plate and  $5\ \mu\text{g}/\text{mL}$  ( $32.8\ \mu\text{mol}/\text{L}$ ) cetuximab,  $2.5\ \mu\text{g}/\text{mL}$  ( $17\ \mu\text{mol}/\text{L}$ ) panitumumab,  $2.5\ \mu\text{g}/\text{mL}$  ( $60\ \mu\text{mol}/\text{L}$ ) 7D12-hcAb, 7D12-E-hcAb, or 7D12-T-hcAb were added. After 15 minutes,  $50\ \mu\text{L}$  active complement containing human serum or  $50\ \mu\text{L}$  complement-inactivated human serum (preheated for 30 minutes at  $56^{\circ}$ ) was added. Cells were incubated for 3 hours at  $37^{\circ}\text{C}$  in a humidified atmosphere with 5%  $\text{CO}_2$ . Lysed cells were stained with Propidium iodid (Becton Dickinson) and dead cells were measured on a FACSCanto (Becton Dickinson).

#### ADCC

Cytotoxicity was analyzed in standard 4 hours  $^{51}\text{Cr}$  release assays performed in 96-well microtiter plates in a total volume of  $200\ \mu\text{L}$  as described (36). Supernatant ( $25\ \mu\text{L}$ ) was mixed with scintillation solution Supermix (Applied Biosystems) and incubated for 15 minutes with agitation.  $^{51}\text{Cr}$  release from triplicates was measured in counts per minute (cpm). Percentage of cellular cytotoxicity was calculated using the formula: % specific lysis =  $(\text{experimental cpm} - \text{basal cpm}) / (\text{maximal cpm} - \text{basal cpm}) \times 100$ . Maximal  $^{51}\text{Cr}$  release was determined by adding Triton X-100 (1% final concentration) to target cells, and basal release was measured in the absence of sensitizing proteins and effector cells. We used a 40:1 effector-to-target ratio in these experiments. Nanobodies 7D12-hcAb, 7D12-T-hcAb, or 7D12-E-hcAb and antibodies cetuximab and panitumumab were used at indicated concentrations. Rituximab and Fc-optimized rituximab-IgG1-DE (S239D and I332E) were produced as described in ref. 37 and were used as control at indicated concentrations.

#### Data evaluation and statistical analysis

Data were plotted using GraphPad Prism version 7.00 (GraphPad Software). Unpaired Student *t* test, one-way or two-way ANOVA (multiple comparison) were applied for statistical evaluation with *P* values being calculated using two-sided tests. Findings were considered statistically significant for  $P < 0.05$  (\*), very significant for  $P < 0.01$  (\*\*), and highly significant for  $P < 0.001$  (\*\*\*). In all experiments, data represent mean  $\pm$  SD of representative or combined experiments performed in triplicates as indicated.

## Results

### Nanobody 7D12-hcAb retains binding to EGFR ectodomain mutations involved in cetuximab or panitumumab resistance

Recent studies have shown that a number of EGFR ectodomain mutations may be acquired on EGFR-directed antibody treatment

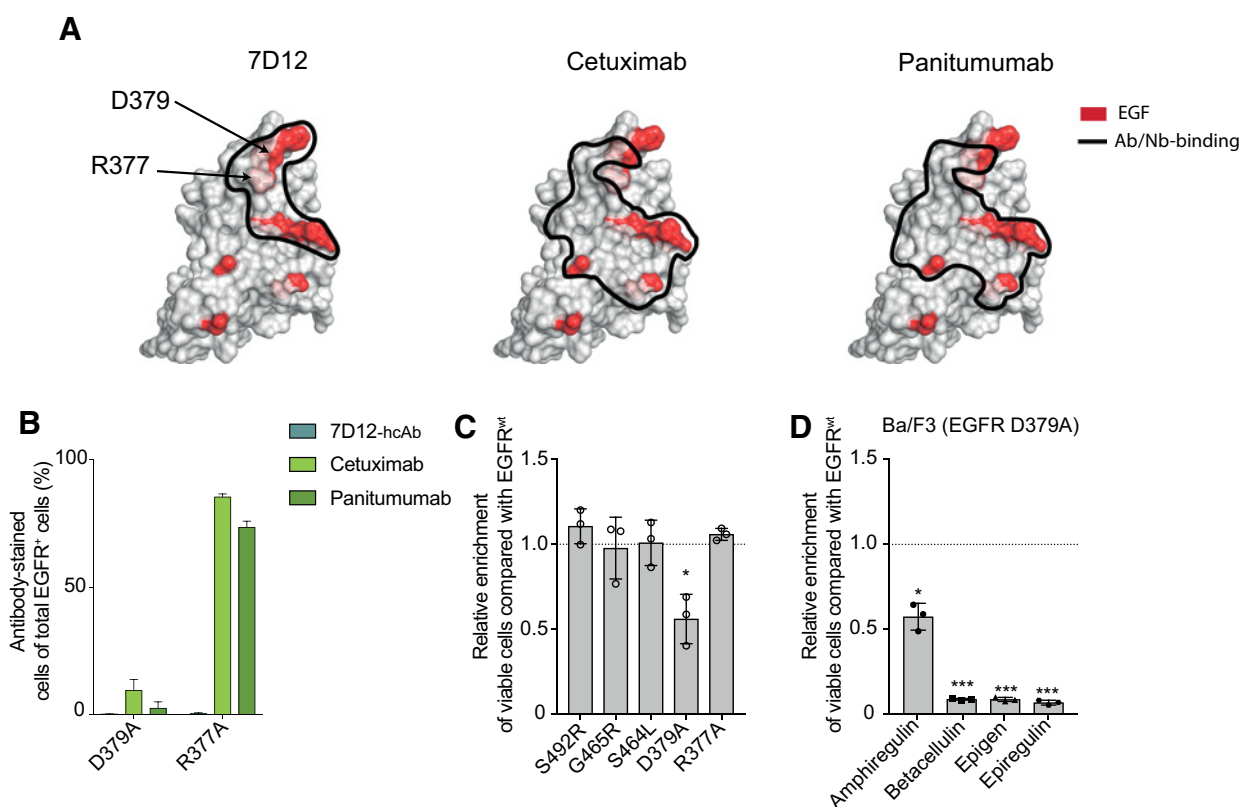
in patients with metastatic colorectal cancer (13). Localized within the binding site of panitumumab and/or cetuximab, these mutations result in loss of antibody binding and thus clinical resistance toward one or both antibodies. The polymorphic variant EGFR R521K lies outside the antibody epitopes, but confers antibody resistance via aberrant glycosylation and subsequent loss of antibody affinity (Fig. 1A; Table 1; ref. 18). In contrast to the large binding interfaces recognized by cetuximab and panitumumab on the EGFR ectodomain, the previously described nanobody 7D12 targets a very small epitope that only marginally overlaps with the binding sites of the licensed therapeutic antibodies, but does not overlap with any of the tested EGFR ectodomain III variants involved in antibody resistance (Fig. 1A; Table 1). We therefore set out to test if nanobody 7D12-hcAb (fused to a human IgG1 Fc portion) binds to any of the mutant EGFR variants associated with acquired antibody resistance. To do so, the murine EGFR-negative, IL3-dependent pro-B cell line Ba/F3 was transduced to stably express human EGFR or mutants thereof. 7D12-hcAb recognized all tested EGFR variants that were ectopically expressed on the transduced Ba/F3 cells, whereas as expected cetuximab only bound the R451C and K467T variant and panitumumab bound the EGFR S492R, I491K, K467T, I462A, R451C, and V441F (Fig. 1B; Table 1).

### 7D12-hcAb kills cells expressing EGFR ectodomain mutations involved in resistance to cetuximab or panitumumab

To evaluate whether apart from binding to EGFR ectodomain mutant cell lines, 7D12-hcAb also inhibits EGF-dependent growth, we established a proliferation assay in Ba/F3 EGFR WT cells. We observed no proliferation in Ba/F3 EGFR WT cells upon treatment with 7D12-hcAb, cetuximab, or panitumumab (Fig. 1C). Moreover, nanobody 7D12-hcAb was able to block growth stimulation of EGFR WT transduced Ba/F3 cells upon stimulation with other EGFR ligands, namely, amphiregulin, betacellulin, epigen, or epiregulin (Supplementary Fig. S1). In line with antibody/nanobody binding results, we only found nanobody 7D12-hcAb to inhibit Ba/F3 EGFR G465R-mutant cell growth in contrast to cetuximab or panitumumab ( $P < 0.001$ ; Fig. 1C). These data suggested that targeting of the 7D12 epitope overcomes resistance acquired on panitumumab and/or cetuximab treatment.

### Secondary resistance to 7D12-Fc can only be mediated by EGFR R377 mutations

Next, we went on to evaluate the risk of secondary resistance development on treatment with 7D12-hcAb. The risk for secondary resistance theoretically increases with the size of the EGFR epitope, because in larger epitopes a more diverse range of single amino acid substitutions may be resulting in abrogated antibody/nanobody binding. In addition, this risk may depend on the functional importance of the targeted amino acid positions, because epitope escape variants will only be selected if receptor functionality is retained in the mutant variant. Compared with the cetuximab and panitumumab epitope, the 7D12-hcAb epitope is much smaller (Fig. 2A). Moreover, it almost completely overlaps with the EGF-binding site on the receptor, suggesting that only few—if any—mutations may abrogate 7D12-hcAb binding while sparing receptor functionality. In contrast, antibodies targeting large epitopes that only partially overlap with the EGF-binding site are expected to be more prone to acquired resistance due to a larger number of functionally intact epitope escape variants. This

**Figure 2.**

Secondary resistance to 7D12-Fc can only be mediated by EGFR R377 mutations. **A**, Schematic overview of antibody or nanobody epitopes relative to the EGF-binding site. EGFR was extracted under accession code 1IVO from Protein Data Bank and EGF, antibody or nanobody binding was extracted from the literature (Table 1). EGF-binding positions were marked red, and antibody/nanobody binding positions were circled. **B**, Binding of nanobody 7D12-hcAb, cetuximab, and panitumumab to synthetic EGFR variants R377A and D379A. EGFR WT, EGFR D379A, or R377A-transduced Ba/F3 cells were fluorescently labeled with either nanobody 7D12-hcAb (blue) therapeutic antibody cetuximab (light green) or panitumumab (dark green) and specific secondary antibody. Relative amount of EGFR<sup>+</sup> cells was determined by gating on vector expressing cells (eGFP<sup>+</sup>) followed by gating on antibody/nanobody-labeled cells. Experiments were performed at least two times in triplicates. Results are presented as mean  $\pm$  SD. **C**, Growth of Ba/F3 cells transduced with EGFR S492R, G465R, S464L, D379A, or R377A. EGFR WT or EGFR-mutant S492R-, G465R-, S464L-, D379A-, or R377A-transduced Ba/F3 cells were seeded in triplicates at equal densities, and the average number of viable cells were measured after trypan blue staining using Vi-CELL. After 72 hours under EGF stimulation, increase of viable cells from indicated EGFR variant was calculated relative to EGFR WT Ba/F3 cells. One experiment out of two to three is shown. Results are presented as mean  $\pm$  SD. **D**, Growth stimulation of EGFR D379A-mutated Ba/F3 cells by EGFR ligands is limited. EGFR WT and EGFR D379A-transduced Ba/F3 cells were seeded in triplicates at equal densities, and the average number of viable cells were measured after trypan blue staining using Vi-CELL. Increase of viable mutant EGFR D379A cells after 72 hours under stimulation with 10 ng/mL amphiregulin, betacellulin, epigen, or epiregulin was calculated relative to EGFR WT Ba/F3 cells. One experiment out of two is shown. Results are presented as mean  $\pm$  SD. Statistical significance was calculated using a one sample *t* test against value 1 (**C** and **D**). \*,  $P < 0.05$ ; \*\*\*,  $P < 0.001$ .

is underlined by the clinical observations of acquired mutations during cetuximab therapy that are located outside of the EGF-binding site such as positions S492, I491, K489, K467, G465, S464, I462, R451, and V441 (13, 16, 18, 38).

In this line of reasoning, we asked if single epitope escape mutations that overlap with the EGF-binding site do result in loss of EGFR functionality. To experimentally test this, Ba/F3 cells were transduced to express the synthetic variant EGFR D379A, affecting a central EGFR residue reported to be involved both in EGF binding as well as in cetuximab, panitumumab, and nanobody 7D12-hcAb binding. As expected, Ba/F3 cells expressing this variant were not bound by any of the therapeutic antibodies nor by the nanobody, and receptor functionality was disrupted as shown by the lack of IL3-independent/EGF-dependent growth (Fig. 2B and C). In addition, EGFR D379A-transduced Ba/F3 cells could not be stimulated with

other EGFR ligands such as amphiregulin, betacellulin, epigen, or epiregulin (Fig. 2D). In contrast, receptor functionality was preserved in all the other EGFR variants (Fig. 2C; Supplementary Fig. S2B). By using anti-EGFR staining in flow cytometry, we could rule out any difference in EGFR surface expression of EGFR variant D379A that would explain EGFR disruption (Supplementary Fig. S2A). Indeed, acquired resistance mutations at this position have not been reported thus far on EGFR-directed treatment, supporting our hypothesis that mutations involving the EGF-binding site would not be selected *in vivo* due to loss of receptor functionality. The only position within the 7D12-hcAb epitope that has not been previously reported to be involved in EGF binding (and could therefore be a possible site for resistance-mediating mutations toward 7D12-hcAb) was position R377 of the EGFR. We reasoned that NGS-assisted phage display would allow us to define the importance of this

position for 7D12-hcAb binding. Specifically, these experiments should predict which amino acid substitution of R377 would lead to abrogation of 7D12-hcAb binding. We therefore subjected 7D12-hcAb to three rounds of biopanning using two different random peptide libraries, one with a cysteine-flanked 7mer peptide, the other with a linear 12mer peptide. As opposed to our positive control antibody rituximab (39), phage enrichments on 7D12-hcAb were weak, no conclusive paratope-binding peptide motif could be deduced and therefore no definition of amino acids in position R377 preventing 7D12-hcAb binding was derived (Supplementary Fig. S3). This suggested that either the discontinuous epitope could not easily be mimicked by the linear peptides or post-translational modifications were of importance in the 7D12-hcAb-epitope interaction. However, to explore the consequences of a very drastic amino acid substitution at EGFR position R377 on 7D12-hcAb and EGF binding, we substituted arginine by alanine, thereby abrogating the positive charge in this position. Ba/F3 cells could be successfully transduced to express this synthetic variant EGFR R377A (Supplementary Fig. S2A). As expected, this mutant retained receptor functionality (Fig. 2C) and resulted in loss of 7D12-hcAb binding (Fig. 2B), indicating that R377 is a predilection site for resistance-mediating mutations toward 7D12-hcAb. Because this site is located outside the cetuximab and panitumumab epitope, we reasoned that these two antibodies would still be able to bind the mutant R377A variant, which could be confirmed by binding experiments (Fig. 2B).

#### EGFR targeting with 7D12-hcAb does not overcome resistance mediated by the EGFR SNP R521K

In about one third of HNSCC patients, EGFR R521K mediates resistance to cetuximab treatment *in vitro* and *in vivo* correlating with decreased survival in patient cohorts (18–21). As opposed to the acquired EGFR variants that lie within the EGFR antibody epitopes and mediate full loss of antibody binding, EGFR R521K does permit residual antibody binding. Due to reduced affinity, however, the antibody is not able to inhibit the EGFR pathway. We previously used human HNSCC cell lines SAT (*EGFR* R521K) and UTSCC-14 (*EGFR* WT) as a model system to study primary cetuximab resistance (18). Our data suggested that cetuximab dosing exceeding the maximum tolerated doses established in clinical trials was able to overcome resistance in this "low-affinity" EGFR variant (18). Because nanobody-Fc fusion proteins are significantly smaller in size than conventional antibodies (42 kDa versus 150 kDa), we were interested if their potentially superior tissue penetration was sufficient to overcome resistance in SAT cells. To test this, we performed experiments in a 3D proliferation model using tumor spheroids generated with both cell lines. We were able to inhibit cellular growth of EGFR WT expressing HNSCC cells (UTSCC-14) by 7D12-hcAb, cetuximab, or panitumumab treatment (Fig. 3). In the SAT spheroid model, we only found moderate growth inhibition by 7D12-hcAb, cetuximab, or panitumumab, suggesting that resistance could not be overcome by use of 7D12-hcAb (Fig. 3).

#### Fc modification enhances 7D12-hcAb complement-dependent and cellular cytotoxicity toward EGFR R521K

Because receptor binding of 7D12-hcAb to EGFR R521K was preserved, we reasoned that resistance could be overcome

by using 7D12-hcAb nanobodies carrying an Fc-modification that enhances immunologic effector functions. This has been previously shown for the Fc-optimized cetugex antibody that showed marked activity against cells expressing the EGFR R521K variant despite inability to inhibit the EGFR pathway (18).

First, we introduced the Fc-mutation E345R into the 7D12-hcAb construct (7D12-E-hcAb). This modification is known to enhance CDC in the antibody context (32). In UTSCC-14 cells, we found higher levels of complement-dependent cell lysis after treatment with 7D12-E-hcAb than with 7D12-hcAb, cetuximab, or panitumumab (Fig. 4A). In EGFR-R521K expressing SAT cells, no lysis was observed with 7D12-hcAb, cetuximab, or panitumumab, but moderate cell lysis was seen if the optimized construct 7D12-E-hcAb was used (Fig. 4A). Consistently, the triple-mutant 7D12-T-hcAb (G236A, S239D, and I332E), which was optimized to enhance ADCC, did not induce stronger complement-dependent lysis than 7D12-hcAb (Fig. 4A; ref. 33). We found comparable results within the Ba/F3 model system using EGFR WT and EGFR R521K-transduced cells, which ruled out cell line differences other than the EGFR variant R521K (Fig. 4B) and in a more natural setting where downstream mutations in KRAS (G12V) simultaneously occur (Fig. 4C).

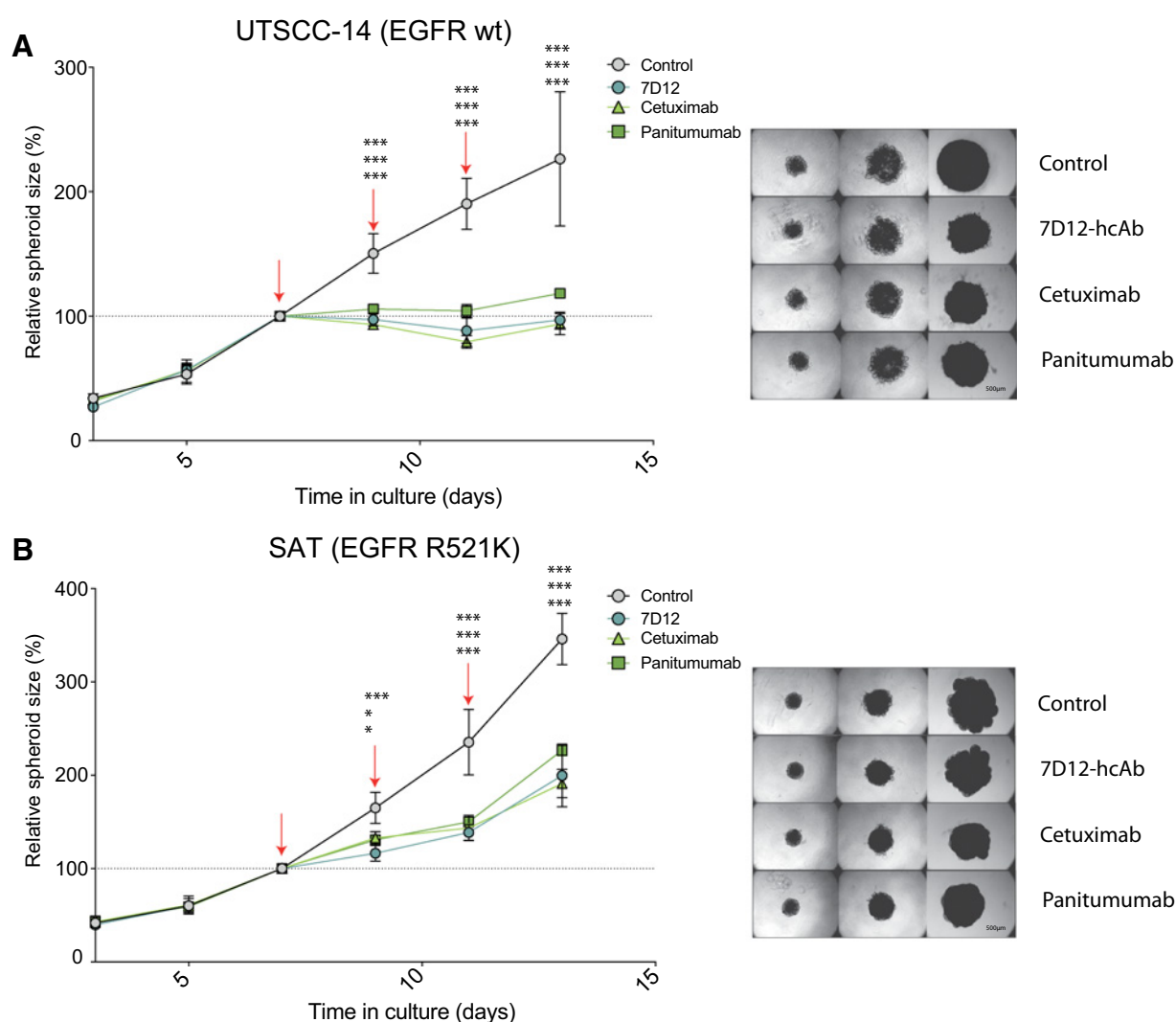
In a second model using NK cells to induce cellular lysis, we were able to demonstrate the superiority of 7D12-T-hcAb in an ADCC-dependent assay (36). As expected, 7D12-hcAb, cetuximab, or panitumumab efficacy was inferior to 7D12-T-hcAb in EGFR WT UTSCC-14 and EGFR R521K SAT cells (Fig. 4D).

Together, 7D12-hcAb is able to bind EGFR ectodomain mutations acquired on EGFR antibody therapy *in vivo* and to block proliferation in cells expressing these variants. Acquired resistance due to EGFR ectodomain mutations toward 7D12-hcAb is limited due to its small epitope and almost full overlap with the EGF-binding site and can eventually be overcome by conventional EGFR antibodies. Overcoming resistance mediated by low-affinity EGFR variants or targeting of EGFR downstream mutated variants is more complex and may require improvements in antibody/nanobody effector functions.

## Discussion

Primary and secondary resistance represents a major challenge in antibody targeting of the EGFR. Recent evidence suggests that in addition to mutations in a number of downstream signaling molecules (e.g., RAS), the EGFR itself may harbor polymorphic variants or acquired point mutations that lead to resistance toward established therapeutic antibodies. To personalize EGFR-directed treatment, we need to gain insight into alternative ways to target this essential pathway. This may include the development of liquid biopsy approaches to monitor for resistant subclones (40, 41), drug holiday strategies to hamper the selection of RAS-mutant subclones (42), and the development of agents with alternative or multiple epitope recognition that may overcome resistance by acquired EGFR ectodomain mutations or that prevent their selection in the first place (22, 43).

In this work, we studied the potential of a nanobody-Fc fusion protein (7D12-hcAb) to target cells expressing EGFR variants involved in primary and acquired resistance to cetuximab or panitumumab. Taken together, our data can be summarized to three major findings: (i) 7D12-hcAb targets EGFR ectodomain mutants selected during cetuximab or panitumumab treatment, thereby representing a potential salvage option after emergence of

**Figure 3.**

7D12-hcAb targeting does not overcome resistance mediated by polymorphism EGFR R521K. Proliferation of human cell lines UTSCC-14 (EGFR WT) and SAT (EGFR R521K) was determined in 3D cellular spheroid model *in vitro*. Cells were grown for 7 days before antibody or nanobody (7D12-hcAb 60  $\mu\text{mol/L}$ ; cetuximab 32.8  $\mu\text{mol/L}$ ; panitumumab 17  $\mu\text{mol/L}$ ) was added every other day (red arrow). Pictures were taken every other day, and spheroid size was calculated using Axiocvert 25 microscope. Statistics show cell size relative to day 7 before initiation of treatment. One representative experiment with representative pictures (from left to right for days 1, 7, and 13 and indicated treatment) out of two to three experiments (performed in triplicates) is shown. Results are presented as mean  $\pm$  SD. Statistical significance was calculated using two-way ANOVA followed by a Dunnett *post hoc* test for multiple comparisons (\*\*\*,  $P < 0.001$ ; \*,  $P < 0.05$ ) and presented from top to bottom for nanobody 7D12-hcAb, panitumumab, and cetuximab at each time point.

acquired resistance. (ii) Given its small epitope that almost completely overlaps with the EGF-binding site, 7D12-hcAb treatment is less likely to induce secondary resistance *in vivo*. On the other hand, if resistance occurs due to mutations in EGFR position R377, these variants can be targeted by conventional EGFR antibodies. (iii) 7D12-hcAb can easily be Fc-optimized for immunologic effector functions that enhance killing of EGFR WT cells, KRAS-mutated cells, and may even allow killing of cells with a "low-affinity" EGFR ectodomain variant.

The first point is extremely relevant because the liquid biopsy technology that allows the monitoring for resistance-mediating mutations is entering clinical practice. Although the majority of EGFR ectodomain mutations mediate resistance toward both licensed EGFR antibodies, 7D12-hcAb has been able to target all

tested epitope escape variants. It may, therefore, close this therapeutic gap and allow for rational drug switching based on mutational status. The feasibility of retargeting EGFR after the occurrence of resistance to cetuximab or panitumumab has been recently addressed using a dual human–mouse chimeric antibody combination with nonoverlapping epitopes on EGFR (Sym004; ref. 23). However, despite the effective targeting of ectodomain-mutated EGFR, a general clinical benefit in overall survival was prevalent only in a RAS and BRAF WT cohort, which might be explained by the overall subclonal nature of ectodomain mutations and the heterogeneity and high prevalence of downstream RAS or BRAF mutations. Here, we show that nanobody 7D12-hcAb might be as effective in targeting ectodomain mutants, but can be further Fc-modified to kill downstream mutated subclones



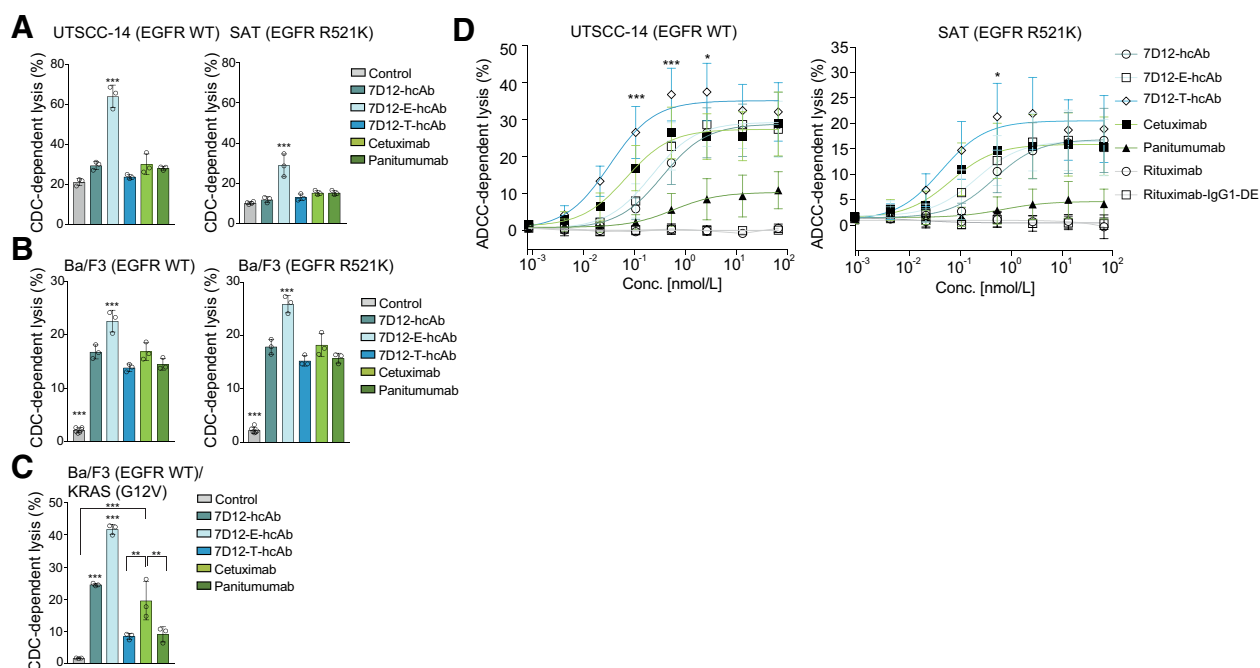


**Figure 4.**

7D12-hcAb can be Fc optimized for CDC or ADCC to enhance activity toward EGFR R521K or KRAS mutated cells. **A**, 7D12-E-hcAb modification (E345R) enhances CDC activity toward EGFR R521K expressing cells. Human cell lines UTSCC-14 (EGFR WT) or SAT (EGFR R521K) were incubated with 60  $\mu\text{mol/L}$  of indicated nanobodies 7D12-hcAb, 7D12-E-hcAb, or 7D12-T-hcAb or 32.8  $\mu\text{mol/L}$  of cetuximab or 17  $\mu\text{mol/L}$  of panitumumab together with human serum or inactivated human serum as control. The number of lysed cells was determined using propidium iodide via flow cytometry. Representative results from one out of two experiments in triplicates are presented as means  $\pm$  SD. **B**, as in **A** except EGFR WT or EGFR R521K Ba/F3 cells were used. **C**, Nanobody 7D12 FC modification (G236A, S239D, I332E) enhances ADCC activity toward cells expressing EGFR R521K. ADCC against human cell lines UTSCC-14 (EGFR WT) or SAT (EGFR R521K) was determined for nanobodies 7D12-hcAb, 7D12-E-hcAb, 7D12-T-hcAb, rituximab, or rituximab-IgG1-DE as described in Materials and Methods. Percentage of lysed cells at indicated concentration is shown. 40:1 effector-to-target ratio was used. Means from five independent experiments are shown, and results are presented  $\pm$  SD. Statistical significance was indicated for 7D12-T-hcAb in comparison with 7D12-hcAb. Statistical significance was calculated using one-/two-way ANOVA followed by a Tukey (**A-C**) or Bonferroni (**D**) *post hoc* test for multiple comparisons (\*\*\*,  $P < 0.001$ ; \*\*,  $P < 0.01$ ; \*,  $P < 0.05$ ).

when pathway inhibition is undermined by *RAS* or *BRAF* mutations using CDC or ADCC. The effectiveness of using Fc-modified antibodies to target *KRAS*-mutated colorectal cancer cells was also proven in mouse xenograft models (44). However, tested antibodies were not optimized to simultaneously target ectodomain variants in contrast to nanobody 7D12 constructs. In comparison, Sym004 leads to efficient pathway inhibition via internalization and downregulation of EGFR (45), which might prevent CDC and ADCC activity and could partly explain the ineffectiveness in unselected patient cohorts. Therefore, these promising data should trigger evaluation of nanobody 7D12-hcAb or—ideally—Fc-optimized versions thereof in future clinical trials that shape our ideas about the real rate of secondary EGFR ectodomain mutations on this agent, the *in vivo* druggability of cetuximab/panitumumab escape variants and the potential effects of optimized 7D12-hcAb on the selection and targeting of *RAS*-mutant subclones. Of course, these trials further need to evaluate whether Fc-modified variants are needed to compensate for its slightly lower affinity to EGFR compared with cetuximab as found in recent studies (27, 28). Clinical studies in other indications already showed a low immunogenicity of nanobodies with limited occurrence of anti-nanobody antibodies due to their large homology with the human VH gene (46), supporting its tolerability and potential clinical value.

Together, nanobody 7D12-hcAb represents a highly interesting potential therapeutic in the quest for more personalized and resistance-preventive targeting of the EGFR pathway.

#### Disclosure of Potential Conflicts of Interest

C. Bokemeyer has received honoraria from speakers bureau of Merck Serono. F. Koch-Nolte reports receiving other commercial research support from antibody sales and has ownership interest (including stock, patents, etc.) in an entity. F. Koch-Nolte is coinventor on nanobody patent applications and receives royalties from sales of antibodies developed in his lab via MediGate GmbH, a 100% subsidiary of the University Medical Center, Hamburg. No potential conflicts of interest were disclosed by the other authors.

#### Authors' Contributions

**Conception and design:** J. Tintelnot, N. Baum, F. Koch-Nolte, M. Binder  
**Development of methodology:** N. Baum, C. Schultheiß, F. Braig, M. Trentmann, J. Finter, P. Bannas, B. Fehse, F. Koch-Nolte  
**Acquisition of data (provided animals, acquired and managed patients, provided facilities, etc.):** J. Tintelnot, N. Baum, C. Schultheiß, M. Trentmann, W. Fumey, K. Riecken, K. Schuetze, C. Bokemeyer, M. Peipp, F. Koch-Nolte  
**Analysis and interpretation of data (e.g., statistical analysis, biostatistics, computational analysis):** J. Tintelnot, N. Baum, J. Finter, P. Bannas, C. Bokemeyer, T. Rösner, F. Koch-Nolte, M. Binder

**Writing, review, and/or revision of the manuscript:** J. Tintelnot, J. Finter, P. Bannas, B. Fehse, K. Riecken, C. Bokemeyer, T. Valerius, M. Peipp, F. Koch-Nolte, M. Binder

**Administrative, technical, or material support (i.e., reporting or organizing data, constructing databases):** J. Tintelnot, N. Baum, F. Braig, P. Bannas, T. Rösner

**Study supervision:** N. Baum

## Acknowledgments

The authors thank Anita Schlenker, Dana Lea Krüger, and Barbara Gösch for technical assistance. We are indebted to the UKE FACS/Sorting Core Unit for

expert support. This project received funding by the German Research Foundation (grant BI1711/1-2 to M. Binder). B. Fehse was supported by German Cancer Aid (111303).

The costs of publication of this article were defrayed in part by the payment of page charges. This article must therefore be hereby marked *advertisement* in accordance with 18 U.S.C. Section 1734 solely to indicate this fact.

Received August 2, 2018; revised November 30, 2018; accepted February 22, 2019; published first March 1, 2019.

## References

- Bonner JA, Harari PM, Giralt J, Azarnia N, Shin DM, Cohen RB, et al. Radiotherapy plus cetuximab for squamous-cell carcinoma of the head and neck. *N Engl J Med* 2006;354:567–78.
- Cunningham D, Humblet Y, Siena S, Khayat D, Bleiberg H, Santoro A, et al. Cetuximab monotherapy and cetuximab plus irinotecan in irinotecan-refractory metastatic colorectal cancer. *N Engl J Med* 2004;351:337–45.
- Douillard JY, Siena S, Cassidy J, Tabernero J, Burkes R, Barugel M, et al. Randomized, Phase III trial of panitumumab with infusional fluorouracil, leucovorin, and oxaliplatin (FOLFOX4) Versus FOLFOX4 alone as first-line treatment in patients with previously untreated metastatic colorectal cancer: The PRIME study. *J Clin Oncol* 2010;28:4697–705.
- Van Cutsem E, Köhne C-H, Hitre E, Zaluski J, Chang Chien C-R, Makhson A, et al. Cetuximab and chemotherapy as initial treatment for metastatic colorectal cancer. *N Engl J Med* 2009;360:1408–17.
- Vermorken JB, Mesia R, Rivera F, Remenar E, Kaweckí A, Rottey S, et al. Platinum-based chemotherapy plus cetuximab in head and neck cancer. *N Engl J Med* 2008;359:1116–27.
- Ciardello F, Tortora G. EGFR antagonists in cancer treatment. *N Engl J Med* 2008;358:1160–74.
- Veluchamy JP, Spanholtz J, Tordoir M, Thijssen VL, Heideman DAM, Verheul HMW, et al. Combination of NK cells and cetuximab to enhance anti-tumor responses in RAS mutant metastatic colorectal cancer. *PLoS One* 2016;11:1–16.
- Schneider-Merck T, Lammerts van Bueren JJ, Berger S, Rossen K, van Berkel PHC, Derer S, et al. Human IgG2 antibodies against epidermal growth factor receptor effectively trigger antibody-dependent cellular cytotoxicity but, in contrast to IgG1, only by cells of myeloid lineage. *J Immunol* 2010;184:512–20.
- Dechant M, Weisner W, Berger S, Peipp M, Beyer T, Schneider-Merck T, et al. Complement-dependent tumor cell lysis triggered by combinations of epidermal growth factor receptor antibodies. *Cancer Res* 2008;68:4998–5003.
- Jamal-Hanjani M, Wilson GA, McGranahan N, Birkbak NJ, Watkins TBK, Veeriah S, et al. Tracking the evolution of non-small-cell lung cancer. *N Engl J Med* 2017;376:2109–21.
- Abbosh C, Birkbak NJ, Wilson GA, Jamal-Hanjani M, Constantin T, Salari R, et al. Phylogenetic ctDNA analysis depicts early-stage lung cancer evolution. *Nature* 2017;545:446–51.
- Braig F, März M, Schieferdecker A, Schulte A, Voigt M, Stein A, et al. Epidermal growth factor receptor mutation mediates cross-resistance to panitumumab and cetuximab in gastrointestinal cancer. *Oncotarget* 2015;6:12035–47.
- Arena S, Bellosillo B, Siravegna G, Martínez A, Cañadas I, Lazzari L, et al. Emergence of multiple EGFR extracellular mutations during cetuximab treatment in colorectal cancer. *Clin Cancer Res* 2015;21:2157–66.
- Montagut C, Dalmases A, Bellosillo B, Crespo M, Pairet S, Iglesias M, et al. Identification of a mutation in the extracellular domain of the Epidermal Growth Factor Receptor conferring cetuximab resistance in colorectal cancer. *Nat Med* 2012;18:221–3.
- Strickler JH, Loree JM, Ahronian LG, Parikh AR, Niedzwiecki D, Pereira AAL, et al. Genomic landscape of cell-free DNA in patients with colorectal cancer. *Cancer Discov* 2018;8:164–73.
- Voigt M, Braig F, Göthel M, Schulte A, Lamszus K, Bokemeyer C, et al. Functional dissection of the epidermal growth factor receptor epitopes targeted by panitumumab and cetuximab. *Neoplasia* 2012;14:1023–31.
- Newhall K, Price T, Peeters M, Kim TW, Li J, Cascinu S, et al. O-0011 \* Frequency of S492R mutations in the epidermal growth factor receptor: analysis of plasma Dna from metastatic colorectal cancer patients treated with panitumumab or cetuximab monotherapy. *Ann Oncol* 2014;25:ii109–ii109.
- Braig F, Kriegs M, Voigtlaender M, Habel B, Grob T, Biskup K, et al. Cetuximab resistance in head and neck cancer is mediated by EGFR-K521polymorphism. *Cancer Res* 2017;77:1188–99.
- Wang Y, Zha L, Liao D, Li X. A meta-analysis on the relations between EGFR R521K polymorphism and risk of cancer. *Int J Genomics* 2014;2014:1–7.
- Stoehlmacher-Williams J, Obermann L, Ehninger G, Goekurt E. Polymorphisms of the epidermal growth factor receptor (EGFR) and survival in patients with advanced cancer of the head and neck (HNSCC). *Anticancer Res* 2012;32:421–5.
- Klinghammer K, Knödler M, Schmittl A, Budach V, Keilholz U, Tinhofer I. Association of epidermal growth factor receptor polymorphism, skin toxicity, and outcome in patients with squamous cell carcinoma of the head and neck receiving cetuximab-docetaxel treatment. *Clin Cancer Res* 2010;16:304–10.
- Kearns JD, Bukhalid R, Sevecka M, Tan G, Gerami-Moayed N, Werner SL, et al. Enhanced targeting of the EGFR network with MM-151, an oligoclonal anti-EGFR antibody therapeutic. *Mol Cancer Ther* 2015;14:1625–36.
- Montagut C, Argilés G, Ciardello F, Poulsen TT, Dienstmann R, Kragh M, et al. Efficacy of Sym004 in patients with metastatic colorectal cancer with acquired resistance to anti-EGFR therapy and molecularly selected by circulating tumor DNA analyses a phase 2 randomized clinical trial. *JAMA Oncol* 2018;4:1–9.
- Hamers-Casterman C, Atarhouch T, Muyldermans S, Robinson G, Hammers C, Songa EB, et al. Naturally occurring antibodies devoid of light chains. *Nature* 1993;363:446–8.
- Van Audenhove I, Gettemans J. Nanobodies as versatile tools to understand, diagnose, visualize and treat cancer. *EBioMedicine* 2016;8:40–8.
- Harmsen MM, De Haard HJ. Properties, production, and applications of camelid single-domain antibody fragments. *Appl Microbiol Biotechnol* 2007;77:13–22.
- Roovers RC, Vosjan MJ, Laeremans T, el Khoulati R, de Bruin RC, Ferguson KM, et al. A bi-paratopic anti-EGFR nanobody efficiently inhibits solid tumour growth. *Int J Cancer* 2011;58:765–98.
- Schmitz KR, Bagchi A, Roovers RC, van Bergen en Henegouwen PM, Ferguson KM. Structural evaluation of EGFR inhibition mechanisms for nanobodies/VHH domains. *Structure* 2013;21:1214–24.
- Bannas P, Hambach J, Koch-Nolte F. Nanobodies and nanobody-based human heavy chain antibodies as antitumor therapeutics. *Front Immunol* 2017;8:1–13.
- Weber K, Bartsch U, Stocking C, Fehse B. A multicolor panel of novel lentiviral "gene ontology" (LeGO) vectors for functional gene analysis. *Mol Ther* 2008;16:698–706.
- Jäger V, Büsow K, Wagner A, Weber S, Hust M, Frenzel A, et al. High level transient production of recombinant antibodies and antibody fusion proteins in HEK293 cells. *BMC Biotechnol* 2013;13.

32. Diebold CA, Beurskens FJ, De Jong RN, Koning RI, Strumane K, Lindorfer MA, et al. Complement is activated by IgG hexamers assembled at the cell surface. *Science* 2014;343:1260–3.
33. Moore GL, Chen H, Karki S, Lazar GA. Engineered Fc variant antibodies with enhanced ability to recruit complement and mediate effector functions. *MAbs* 2010;2:181–9.
34. Danquah W, Meyer-Schwesinger C, Rissiek B, Pinto C, Serracant-Prat A, Amadi M, et al. Nanobodies that block gating of the P2X7 ion channel ameliorate inflammation. *Sci Transl Med* 2016;8:366ra162.
35. Frith MC, Saunders NFW, Kobe B, Bailey TL. Discovering sequence motifs with arbitrary insertions and deletions. *PLoS Comput Biol* 2008;4:e1000071.
36. Kellner C, Hallack D, Glorius P, Staudinger M, Mohseni Nodehi S, De Weers M, et al. Fusion proteins between ligands for NKG2D and CD20-directed single-chain variable fragments sensitize lymphoma cells for natural killer cell-mediated lysis and enhance antibody-dependent cellular cytotoxicity. *Leukemia* 2012;26:830–4.
37. Kellner C, Derer S, Klausz K, Roskopf S, Wirt T, Rösner T, et al. Fc glyco- and Fc protein-engineering: design of antibody variants with improved ADCC and CDC activity. In: Damien Nevoltris PC, editor. *Antibody engineering*. 3rd ed. Totowa, NJ: Humana Press; 2018.
38. Li S, Kussie P, Ferguson KM. Structural basis for EGF receptor inhibition by the therapeutic antibody IMC-11F8. *Structure* 2008;16:216–27.
39. Binder M, Otto F, Mertelsmann R, Veelken H, Trepel M. The epitope recognized by rituximab. *Blood* 2006;108:1975–8.
40. Trojan J, Klein-Scory S, Koch C, Schmiegel W, Baraniskin A. Clinical application of liquid biopsy in targeted therapy of metastatic colorectal cancer. *Case Rep Oncol Med* 2017;2017:1–3.
41. Thierry AR, Pastor B, Jiang Z-Q, Katsiampoura AD, Parseghian C, Loree JM, et al. Circulating DNA demonstrates convergent evolution and common resistance mechanisms during treatment of colorectal cancer. *Clin Cancer Res* 2017;23:4578–91.
42. Kasper S, Reis H, Ziegler S, Nothdurft S, Mueller A, Goetz M, et al. Molecular dissection of effector mechanisms of RAS-mediated resistance to anti-EGFR antibody therapy. *Oncotarget* 2017;8:45898–917.
43. Napolitano S, Martini G, Martinelli E, Belli V, Laukkanen MO, Sforza V, et al. Therapeutic efficacy of SYM004, a mixture of two anti-EGFR antibodies in human colorectal cancer with acquired resistance to cetuximab and MET activation. *Oncotarget* 2017;8:67592–604.
44. Gerdes CA, Nicolini VG, Herter S, Van Puijnenbroek E, Lang S, Roemmele M, et al. GA201 (RG7160): a novel, humanized, glycoengineered anti-EGFR antibody with enhanced ADCC and superior in vivo efficacy compared with cetuximab. *Clin Cancer Res* 2013;19:1126–38.
45. Pedersen MW, Jacobsen HJ, Koefoed K, Hey A, Pyke C, Haurum JS, et al. Sym004: A novel synergistic anti-epidermal growth factor receptor antibody mixture with superior anticancer efficacy. *Cancer Res* 2010;70:588–97.
46. Steeland S, Vandenbroucke RE, Libert C. Nanobodies as therapeutics: Big opportunities for small antibodies. *Drug Discov Today* 2016;21:1076–113.
47. Ogiso H, Ishitani R, Nureki O, Fukai S, Yamanaka M, Kim JH, et al. Crystal structure of the complex of human epidermal growth factor and receptor extracellular domains. *Cell* 2002;110:775–87.
48. Li S, Schmitz KR, Jeffrey PD, Wiltzius JJW, Kussie P, Ferguson KM. Structural basis for inhibition of the epidermal growth factor receptor by cetuximab. *Cancer Cell* 2005;7:301–11.
49. Chao G, Cochran JR, Dane Witttrup K. Fine epitope mapping of anti-epidermal growth factor receptor antibodies through random mutagenesis and yeast surface display. *J Mol Biol* 2004;342:539–50.
50. Santra M, Reed CC, Iozzo R V. Decorin binds to a narrow region of the epidermal growth factor (EGF) receptor, partially overlapping but distinct from the EGF-binding epitope. *J Biol Chem* 2002;277:35671–81.